Modern Physics Letters A

IMPLEMENTATION OF THE ATLAS-CONF-2020-002 ANALYSIS IN THE MADANALYSIS 5 FRAMEWORK

TAYLOR MURPHY

Department of Physics, The Ohio State University
191 W. Woodruff Ave., Columbus, OH 43210, U.S.A.
murphy.1573@osu.edu

We present the implementation in MadAnalysis 5 of ATLAS-CONF-2020-002, a search for new phenomena in final states with large jet multiplicities and missing transverse momentum, and detail the validation of this implementation. This ATLAS analysis targets new particles decaying into eight or more jets and significant missing transverse energy ($E_{\mathrm{T}}^{\mathrm{miss}}$) using $\mathcal{L} = 139\,\mathrm{fb}^{-1}$ of proton-proton (pp) collisions at the LHC at a center-of-mass energy of $\sqrt{s} = 13\,\mathrm{TeV}$. We validate our implementation by computing limits on a benchmark supersymmetric model in which pair-produced gluinos decay with unit branching fraction to a pair of top quarks and a neutralino ($pp \to \tilde{g}\tilde{g}$, $\tilde{g} \to t\bar{t} + \tilde{\chi}_1^0$). We find acceptable agreement with the limits on this model provided by ATLAS.

Keywords: Multijet events, supersymmetric models, top-philic new physics

1. Introduction

The second run of the Large Hadron Collider (LHC) has produced an integrated luminosity of $\mathcal{L} \approx 140\,\mathrm{fb}^{-1}$ of proton-proton (pp) collisions at a center-of-mass energy of $\sqrt{s} = 13\,\mathrm{TeV}$. The excellent performance of the LHC, alongside increasingly sophisticated analysis by the ATLAS and CMS collaborations, offers an unprecedented opportunity to explore physics beyond the Standard Model (bSM) — particularly complex scenarios with high jet multiplicities and significant amounts of missing transverse energy ($E_{\mathrm{T}}^{\mathrm{miss}}$). Supersymmetry (SUSY), which remains a leading candidate for bSM physics, can be realized in a panoply of models featuring cascade decays of heavy new species to SM particles alongside invisible light (and possibly stable) new particles. Some such models are expected to produce signatures at the LHC consisting not only of large numbers of jets but also of large-radius jets with masses greater than that of the top quark ($m_t \approx 175\,\mathrm{GeV}$), in stark contrast to SM multijet signatures.

The ATLAS collaboration has published a search for new phenomena producing signatures of this class in a report initially designated as ATLAS-CONF-2020-002.[1] This search requires at least eight jets and imposes additional requirements on b-tagged jets and large-radius jets while vetoing isolated electrons and muons. ATLAS reports no evidence for physics beyond the Standard Model from this search, and

interprets results in the context of three simplified models of gluino pair production, $pp \to \tilde{g}\tilde{g}$, with each gluino decaying to some set of SM particles in addition to an invisible particle inspired by the lightest neutralino $\tilde{\chi}_1^0$ in models where it is the lightest supersymmetric particle (LSP). ATLAS is able to extend lower limits on the gluino mass $m_{\tilde{g}}$ in these models to 1.5–2.0 TeV, with improvements in all cases of several hundred GeV over similar Run 1 analyses.

As we alluded to above, there are many models featuring pair production of heavy (s)particles with subsequent cascade decays to both light- and heavy-flavor quarks and missing energy. In particular, models of new physics that enhance the LHC production of four top quarks ($t\bar{t}t\bar{t}$) are quite common. One well motivated example is the family of models with "supersoft" D-term SUSY breaking and (pseudo-)Dirac gauginos, which predict copious pair production of color-octet scalars (*sgluons*) decaying with varying branching fractions to $t\bar{t}$.[2] In these models, there are regions of parameter space where the sgluon-mediated production of four top quarks is kinematically distinct from SM four-top production and is well suited to be probed by multijet + $E_{\mathrm{T}}^{\mathrm{miss}}$ searches like ATLAS-CONF-2020-002.[3] This is just one example of how it is in the community's interest to be able to interpret this analysis in models not considered by ATLAS. The MadAnalysis 5 framework, which provides a platform to emulate each step of an LHC analysis from detector simulation and object reconstruction to event selection, makes this goal achievable.[4,5] In this note, we describe how we have implemented the ATLAS-CONF-2020-002 analysis in this framework in order to apply it to arbitrary models of new physics.

This note is organized as follows. In Section 2, we reproduce the salient details of the ATLAS-CONF-2020-002 analysis, including object definitions and event selection, and we explain how we have emulated this analysis in the MadAnalysis 5 framework. We present the validation of our implementation in Section 3, describing the simulation of events in one benchmark model of gluino pair production and providing a comparison between limits on this model derived from MadAnalysis 5 to those published by the ATLAS collaboration. We demonstrate good agreement between our results and the most closely comparable ATLAS results. We summarize this note and look forward to future work in Section 4.

2. Description of the analysis

ATLAS-CONF-2020-002 looks for new phenomena in final states with large numbers of jets and significant missing transverse energy. It particularly targets events with at least eight anti-k_t radius $R = 0.4$ jets with transverse momentum $p_{\mathrm{T}} > 50$ GeV or higher, depending on signal region. It also requires a high missing transverse energy significance $\mathcal{S}(E_{\mathrm{T}}^{\mathrm{miss}})$ in order to disambiguate genuine $E_{\mathrm{T}}^{\mathrm{miss}}$ associated with non-interacting particles from specious missing energy due to mismeasurements and fluctuations. This search vetoes virtually all leptons surviving an overlap-removal procedure. The final noteworthy element of this search is a set of cuts on the cumulative mass M_{J}^{Σ} of high-p_{T} large-radius (anti-k_t radius $R = 1.0$) jets, which is

Criterion	Electrons	Muons	Photons	Jets	b-tagged jets
p_{T} [GeV]	> 7.0	> 6.0	> 40	> 20 $[R = 0.4]$ > 100 $[R = 1.0]$	> 20
$\lvert\eta\rvert$	< 2.47	< 2.7	< 2.37 and $\notin (1.37, 1.52)$	< 2.8 $[R = 0.4]$ < 1.5 $[R = 1.0]$	< 2.5

Table 1: Summary of preselection criteria, reproduced in part from Section 4 of ATLAS-CONF-2020-002.[1]

intended to stringently control the SM multijet background. Here we discuss these criteria in some more detail and offer notes about our implementation of this analysis in MadAnalysis 5.

2.1. *Object definitions*

ATLAS-CONF-2020-002 comprises a multi-bin and a single-bin subanalysis, the latter of which defines eight non-overlapping signal regions. We have implemented the single-bin subanalysis in MadAnalysis 5. The signal object candidates are required to satisfy several kinematic criteria and to pass a multi-step procedure for overlap removal. The most important preselection criteria are summarized in Table 1, but we comment more on particle reconstruction here.

Jets are reconstructed using the anti-k_t algorithm[6] and are clustered twice. The primary collection of jets has anti-k_t radius parameter $R = 0.4$. These jets must have transverse momentum $p_{\mathrm{T}} > 20\,\mathrm{GeV}$ and pseudorapidity $|\eta| < 2.8$, except for the calculation of missing transverse energy, $E_{\mathrm{T}}^{\mathrm{miss}}$, for which the latter constraint is relaxed to $|\eta| < 4.5$. There is a second collection of large-radius ("fat") jets with radius parameter $R = 1.0$, $p_{\mathrm{T}} > 100\,\mathrm{GeV}$, and $|\eta| < 1.5$. Narrow $R = 0.4$ jets with $|\eta| < 2.5$ containing b-hadrons are identified as b-tagged jets if the discriminant output of a multivariate algorithm exceeds a threshold resulting in an average b-jet identification efficiency of 70%.

Leptons are subject to relatively mild kinematic requirements. Baseline electrons must have $p_{\mathrm{T}} > 7\,\mathrm{GeV}$ and $|\eta| < 2.47$, and baseline muons must satisfy $p_{\mathrm{T}} > 6\,\mathrm{GeV}$ and $|\eta| < 2.7$. The minimum transverse momentum requirements are raised to $p_{\mathrm{T}} > 20\,\mathrm{GeV}$ for signal electrons and signal muons. These objects are used in leptonic control regions; virtually all baseline leptons are ultimately vetoed in all eight signal regions.

Photons are required to satisfy $p_{\mathrm{T}} > 40\,\mathrm{GeV}$ and $|\eta| < 2.37$. An additional pseudorapidity "crack" veto, $|\eta| \notin (1.37, 1.52)$, is applied to avoid a region of the calorimeter with limited instrumentation.

An overlap-removal procedure is applied to the baseline objects described above in order to resolve reconstruction ambiguities. First, any electron sharing an inner detector track with a muon is rejected. Next, photons with angular distance $\Delta R < 0.4$

from any lepton are discarded. ATLAS uses a standard definition of angular distance,

$$\Delta R = \sqrt{(\Delta y)^2 + (\Delta\phi)^2} \quad \text{with} \quad y = \frac{1}{2}\ln\frac{E+p_z}{E-p_z},$$

in which the rapidity y is defined in terms of the energy E and component p_z of momentum along the beam direction, and ϕ is the azimuthal angle about the beam (z) axis. Following the photon removal, non-b-tagged jets are rejected if closer than $R = 0.2$ to an electron. Finally, leptons within $\Delta R = 0.4$ of a surviving jet are removed, and then jets closer than $\Delta R = 0.4$ to any photon are eliminated. We have implemented all the criteria explicitly mentioned here in the MadAnalysis 5 framework, but it should be noted that there are some additional overlap removal criteria, including *e.g.* restrictions on the number of jet tracks and electron p_{T} ordering, that are not implemented.

The missing transverse energy, $E_{\mathrm{T}}^{\mathrm{miss}}$, is defined as the magnitude of the negative vector sum of the transverse momenta of all signal candidates that pass the overlap removal procedure:

$$E_{\mathrm{T}}^{\mathrm{miss}} = \left| -\sum_i \left[\vec{p}_{\mathrm{T}i}^{\,\mathrm{jet}} + \vec{p}_{\mathrm{T}i}^{\,\mathrm{electron}} + \vec{p}_{\mathrm{T}i}^{\,\mathrm{muon}} + \vec{p}_{\mathrm{T}i}^{\,\mathrm{photon}} \right] \right|.$$

Whereas often a selection cut is imposed on the magnitude of $E_{\mathrm{T}}^{\mathrm{miss}}$, ATLAS-CONF-2020-002 requires a minimum missing transverse energy significance $\mathcal{S}(E_{\mathrm{T}}^{\mathrm{miss}})$. This object is designed to distinguish transverse momentum carried by non-interacting particles from $E_{\mathrm{T}}^{\mathrm{miss}}$ that should be attributed elsewhere. ATLAS has begun to use an "object-based" definition of $\mathcal{S}(E_{\mathrm{T}}^{\mathrm{miss}})$, based on the kinematic qualities and resolutions of each object in an event, given by[7]

$$\mathcal{S}(E_{\mathrm{T}}^{\mathrm{miss}}) = \frac{E_{\mathrm{T}}^{\mathrm{miss}}}{\sqrt{\sigma_{\mathrm{L}}^2(1-\rho_{\mathrm{LT}}^2)}},$$

where σ_{L} is the total expected longitudinal resolution of all objects in the event as a function of the p_{T} of each object, and ρ_{LT} is the correlation factor between all longitudinal and transverse object resolutions. This definition of $\mathcal{S}(E_{\mathrm{T}}^{\mathrm{miss}})$ outputs a pure number, which ATLAS-CONF-2020-002 requires to exceed 5.0. Unfortunately, this measure of $\mathcal{S}(E_{\mathrm{T}}^{\mathrm{miss}})$ cannot to our knowledge be implemented in MadAnalysis 5 at this time. In keeping with some validated implemented searches available on the MadAnalysis 5 Public Analysis Database (PAD)[8] that have confronted this same problem, we have used a $\mathcal{S}(E_{\mathrm{T}}^{\mathrm{miss}})$ proxy,

$$\mathcal{S}_{\mathrm{proxy}}(E_{\mathrm{T}}^{\mathrm{miss}}) = \frac{E_{\mathrm{T}}^{\mathrm{miss}}}{\sqrt{H_{\mathrm{T}}}} \quad \text{with} \quad H_{\mathrm{T}} = \sum_i p_{\mathrm{T}i}^{\mathrm{jet}}, \tag{1}$$

which was used by ATLAS prior to the adoption of the new object-based definition.[9] This proxy has units of $\mathrm{GeV}^{1/2}$, so our cut is at $\mathcal{S}_{\mathrm{proxy}}(E_{\mathrm{T}}^{\mathrm{miss}}) = 5\,\mathrm{GeV}^{1/2}$.

Selection criterion	Selection ranges
Jet multiplicity, N_{jet}	$N_{\text{jet}}^{50} \geq \{8, 9, 10, 11, 12\}$ $N_{\text{jet}}^{80} \geq 9$
Trigger thresholds	6 or 7 jets, $E_{\text{T}} > 45\,\text{GeV}$ 5 jets, $E_{\text{T}} > 65$ or $70\,\text{GeV}$
Lepton veto	0 baseline leptons, $p_{\text{T}} > 10\,\text{GeV}$
$E_{\text{T}}^{\text{miss}}$ significance, $\mathcal{S}(E_{\text{T}}^{\text{miss}})$	$\mathcal{S}(E_{\text{T}}^{\text{miss}}) > 5.0$

Table 2: Summary of common selection criteria, reproduced in part from Sections 4 and 5 and Table 1 of ATLAS-CONF-2020-002.[1] Variable trigger thresholds depend on year in which data were collected.

2.2. *Event selection*

Selection cuts significantly more stringent than the preselection criteria are applied in the eight non-overlapping signal regions of ATLAS-CONF-2020-002. All selection cuts other than those on jet multiplicity and cumulative fat-jet mass are applied to all signal regions. The common cuts are summarized in Table 2. All baseline leptons surviving the overlap-removal procedure with $p_{\text{T}} > 10\,\text{GeV}$ — which include the vast majority of leptons — are rejected to control background from the SM processes $W \to \nu_\ell \ell$, which produce copious $E_{\text{T}}^{\text{miss}}$. Biases in $E_{\text{T}}^{\text{miss}}$ due to pile-up effects are accounted for by removing events containing jets azimuthally separated from $E_{\text{T}}^{\text{miss}}$ by $|\Delta\phi(\text{jet}, E_{\text{T}}^{\text{miss}})| > 2.2$. Standard baseline jets are promoted to signal jets if they have $p_{\text{T}} > 50\,\text{GeV}$ or $> 80\,\text{GeV}$, depending on signal region. All signal jets must have $|\eta| < 2.0$. The final common criterion is the minimum missing transverse energy significance: $\mathcal{S}(E_{\text{T}}^{\text{miss}}) > 5.0$ ($5.0\,\text{GeV}^{1/2}$ if using $\mathcal{S}_{\text{proxy}}(E_{\text{T}}^{\text{miss}})$; see Section 2.1 above).

Once the common criteria are applied, ATLAS-CONF-2020-002 finally imposes unique restrictions on jets to define each signal region in the single-bin analysis. These signal region criteria are summarized in Table 3. The signal regions labeled by `SR-`N_{jet}^{50}`ij50-...` require the presence of at least N_{jet}^{50} jets with $p_{\text{T}} > 50\,\text{GeV}$, where $N_{\text{jet}}^{50} \in [8, 12]$. The first five of these signal regions further require the cumulative mass of the fat jets,

$$M_{\text{J}}^{\Sigma} = \sum_j m_j^{R=1.0},$$

to equal or exceed 340 GeV or 500 GeV depending on signal region. Two of these signal regions finally require nonzero numbers of b-tagged jets. The signal region `SR-9ij80` instead requires at least nine signal jets with $p_{\text{T}} > 80\,\text{GeV}$. We note here that the common $E_{\text{T}}^{\text{miss}}$ significance cut is imposed after the specific jet multiplicity and mass cuts in each signal region.

We have written code in C++ that can be run in the reconstruction (`-R`) mode of MadAnalysis 5 to emulate the analysis described above and allow us

Signal region	N_{jet}^{50}	N_{jet}^{80}	$N_{b\text{-jet}}$	M_{J}^{Σ} [GeV]
SR-8ij50-0ib-MJ500	≥ 8	-	-	≥ 500
SR-9ij50-0ib-MJ340	≥ 9	-	-	≥ 340
SR-10ij50-0ib-MJ340	≥ 10	-	-	≥ 340
SR-10ij50-0ib-MJ500	≥ 10	-	-	≥ 500
SR-10ij50-1ib-MJ500	≥ 10	-	≥ 1	≥ 500
SR-11ij50	≥ 11	-	-	-
SR-12ij50-2ib	≥ 12	-	≥ 2	-
SR-9ij80	-	≥ 9	-	-

Table 3: Summary of signal region criteria for single-bin selections, which appears in Table 3 of ATLAS-CONF-2020-002.[1] A dash (-) indicates that no requirement is applied to the corresponding variable. The requirement $\mathcal{S}(E_{\text{T}}^{\text{miss}}) > 5.0$ is applied to all bins.

to apply it to new event samples. Either for the purpose of validation, which is discussed in Section 3, or in order to analyze different models, we provide as input to MadAnalysis 5 some sample of hard-scattering events that have been matched to parton showers and hadronized. These showered and hadronized events are first passed by MadAnalysis 5 to Delphes 3 version 3.4.2[10,11] and FastJet version 3.3.3,[12] which respectively model the response of the ATLAS detector and perform object reconstruction. For this implementation, we use the Delphes 3 card for the ATLAS detector shipped with MadAnalysis 5 modified to include a collection of jets for both anti-k_t radius parameters ($R = 0.4$ and $R = 1.0$) required for this search. The b-jet tagging algorithm in this default card is left unmodified. The reconstructed events are then analyzed by our reimplementation code, after which MadAnalysis 5 computes the acceptance of the event sample by the emulated selection criteria. With the acceptance(s) in hand, MadAnalysis 5 uses the CLs prescription[13] to compute the expected and observed upper limits at 95% confidence level (CL) on the number of signal events given the official numbers of expected background events and observed events. It can also extrapolate these limits to higher integrated luminosities, assuming no excess is found, with multiple approaches to background error propagation available to the user.[5]

3. Validation

ATLAS-CONF-2020-002 does not provide detailed event yields for each selection cut in any signal region of the single-bin subanalysis, so our implementation is not currently validated in that fashion (but this situation may be remedied in

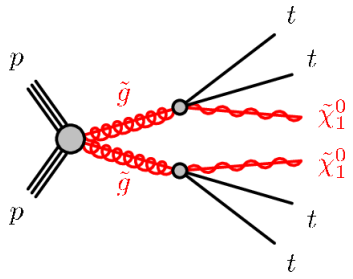

FIG. 1: Diagram representing the signal process $pp \to \tilde{g}\tilde{g}$, $\tilde{g} \to t\bar{t} + \tilde{\chi}_1^0$; which appears in Figure 1(b) of ATLAS-CONF-2020-002.[1] We simulate this process and compute limits in the $(m_{\tilde{g}}, m_{\tilde{\chi}_1^0})$ plane in order to validate our implementation of the analysis.

the medium-term future; see the concluding remarks). ATLAS instead interprets the results of this search in the context of several simplified models inspired by supersymmetry. One of these is a model of gluino pair production, $pp \to \tilde{g}\tilde{g}$, in which each gluino undergoes an effective three-body decay to two top quarks, $t\bar{t}$, and a neutralino, $\tilde{\chi}_1^0$, which is assumed not only electrically neutral but stable at least on collider timescales. This decay is assigned unit branching fraction and is mediated by a highly off-shell squark $\tilde{q}$ with mass $m_{\tilde{q}} \gg m_{\tilde{g}}$. A diagram provided by ATLAS representing this process is reproduced in Figure 1. We validate our implementation by comparing limits on this simplified model derived from MadAnalysis 5 to those reported by ATLAS.

3.1. *Event generation*

There is a simplified model of supersymmetric quantum chromodynamics[14] that was implemented in the Mathematica© package FeynRules,[15–17] whose UFO output is publicly available on the FeynRules model database, that is well suited to simulate the signal events needed to validate our implementation. We have modified this UFO to provide the desired three-body gluino decay $\tilde{g} \to t\bar{t} + \tilde{\chi}_1^0$ with unit branching fraction. In our modified model, the decay is mediated by two stop squarks $\tilde{t}_{\rm L}$ and $\tilde{t}_{\rm R}$ that are decoupled from the low-energy theory with masses $m_{\tilde{t}_{\rm L}} = 9.0\,\text{TeV}$ and $m_{\tilde{t}_{\rm R}} = 8.0\,\text{TeV}$. We use this UFO to simulate events in version 3.1.0 of MadGraph5_aMC@NLO (MG5_aMC).[18,19]

We use MG5_aMC to generate 10^4 events with hard-scattering amplitudes computed at leading order (LO) in the strong coupling for a variety of points in the $(m_{\tilde{g}}, m_{\tilde{\chi}_1^0})$ plane. We convolve these hard-scattering amplitudes with the NNPDF 2.3 LO set of parton distribution functions,[20] fixing the renormalization and factorization scales to the average transverse mass of the final-state particles. The hard-scattering results are matched to parton showers with the aid of Pythia 8 version 8.244,[21] which also simulates hadronization. We then pass these showered and hadronized event samples to MadAnalysis 5 to initiate the analysis process described at the

end of Section 2.2.

The normalization of the event samples passed to MadAnalysis 5 is carried out in a peculiar but well intentioned manner. ATLAS explains that the official samples are normalized to the cross sections of gluino pair production at approximate next-to-next-to-leading order (NNLO) in QCD, including soft gluon emission resummation at next-to-next-to-leading-logarithmic (NNLL) accuracy.[22,23] These cross sections appear to be computed using the program NNLL-fast, which employs the PDF4LHC15_mc NLO PDF set and fixes the renormalization and factorization scales to the average mass of the final-state particles.[24,25] This program requires as input not only the mass $m_{\tilde{g}}$ of the pair-produced gluino, but also the mass $m_{\tilde{q}}$ of a squark. We find variations of factors of $\mathcal{O}(1)$ fb with varying input $m_{\tilde{q}}$, which furthermore cannot be taken high enough to be consistent with the mass of the squark(s) mediating the gluino decay. This is not consistent with the behavior of our signal model. In order to circumvent this issue, and since ATLAS offers no further comment on sample normalization, we scale the LO cross sections computed for our model in MG5_aMC by the K factors (NNLO + NNLL enhancement factors) produced by NNLL-fast and quoted in the associated reference, which we find are almost independent of the input squark mass.[24] These K factors are considerable, ranging from around 2.4 to 2.6, and the cross sections are ultimately of $\mathcal{O}(10)$ fb for gluinos of mass $m_{\tilde{g}} \in (1.4, 1.6)$ TeV. We also use the relatively stable scale and PDF variations output by NNLL-fast to estimate the error in the cross section at the higher order(s) in QCD. These errors are around 5–10% of the cross sections, which amounts to a sizable improvement upon error in the LO cross sections closer to 30%.

3.2. *Comparison with official results*

A comparison of our results and the official $\tilde{g} \to t\bar{t} + \tilde{\chi}_1^0$ benchmark model limits at 95% CL is available in Figure 2. ATLAS provides the limits derived from the multi-bin analysis in Figure 10(b) of ATLAS-CONF-2020-002; the limits from the single-bin analysis are provided in supplementary material. We display in green the expected limits derived from our implementation in MadAnalysis 5, which should be compared only to the expected limits from ATLAS' single-bin analysis. The green band around our expected limit reflects our signal error estimate, given by the sum in quadrature,

$$\delta_{\text{scale}} \oplus \delta_{\text{PDF}} \equiv \left[\delta_{\text{scale}}^2 + \delta_{\text{PDF}}^2\right]^{1/2},$$

of the scale and PDF variations $\delta_{\text{scale}}, \delta_{\text{PDF}}$ discussed above. For this implementation we achieve errors of $\mathcal{O}(10)$ GeV (up to around 50 GeV in either direction) in our expected limits at 95% CL. While these are not displayed, we find similar levels of agreement between our observed limits and ATLAS' single-bin observed limits. We suspect that the largest sources of error are our implementation of the cut on $E_{\text{T}}^{\text{miss}}$ significance and our use of an almost-standard Delphes card, which impacts the detector parametrization, the b-jet tagging algorithm, and the handling of the fat

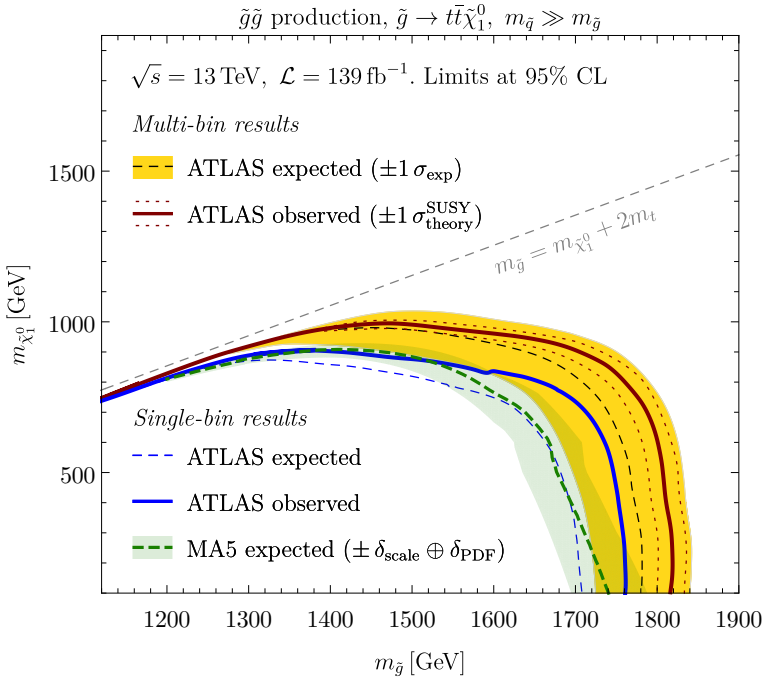

FIG. 2: Exclusion limits at 95% CL on gluino pair production in the $(m_{\tilde{g}}, m_{\tilde{\chi}_1^0})$ plane, assuming gluino decays to $t\bar{t} + \tilde{\chi}_1^0$ via a virtual squark $\tilde{q}$. Multi-bin ATLAS results appear in Figure 10(b) of ATLAS-CONF-2020-002.[1] Single-bin ATLAS results appear in supplementary material for this report. Green exclusion curve traces expected limit derived from our implementation of the single-bin subanalysis. Green shaded band reflects signal error given by sum in quadrature of scale and PDF variations.

jets. Nevertheless, we consider the agreement good enough to claim validation.

4. Conclusions

We have presented the implementation in MadAnalysis 5 of ATLAS-CONF-2020-002, a search for new phenomena in final states with large jet multiplicities and significant missing transverse energy. This analysis can be used to constrain models of new physics featuring multijet signatures, including *e.g.* supersymmetric models predicting $t\bar{t}t\bar{t}$ production with kinematic structure distinct from the analogous SM process. We have validated our implementation by simulating the pair production of gluinos decaying to $t\bar{t}+\tilde{\chi}_1^0$ via a highly off-shell squark — a simplified SUSY-inspired model considered by the ATLAS collaboration in its report — and comparing the expected limits at 95% CL on this model derived from MadAnalysis 5 to those reported by ATLAS. We find acceptable agreement between our results and

the expected limits from the ATLAS single-bin analysis. The DELPHES (detector simulation) and MADANALYSIS recasting cards are available on the MADANALYSIS 5 Public Analysis Database (PAD).

We conclude by noting that ATLAS-CONF-2020-002 has been superseded by an analysis designated as ATLAS-SUSY-2018-17, which — while consisting of the same event definitions and selection strategy and being applied to the same simplified models — boasts the important advantage over ATLAS-CONF-2020-002 of detailed event yields and efficiencies in each signal region for a model of gluino pair production followed by a two-step decay to quarks, W and Z bosons, and $\tilde{\chi}_1^0$. This version of this analysis is an ideal candidate for implementation in MADANALYSIS 5, and a natural extension of this work, so such an implementation is underway.

Acknowledgments

This work was supported in part by the United States Department of Energy under grant DE-SC0011726. The implementation described in this note was used in a paper[3] written by the author of this note in collaboration with L. M. Carpenter and M. J. Smylie. This note shares some text with that document. The importance of their contributions cannot be overstated.

References

1. ATLAS Collaboration, G. Aad *et al.*, *JHEP* **10**, 062 (2020).
2. L. M. Carpenter, T. Murphy and M. J. Smylie, *JHEP* **11**, 024 (2020).
3. L. M. Carpenter, T. Murphy and M. J. Smylie, `arXiv:2107.13565` (2021).
4. E. Conte, B. Dumont, B. Fuks and C. Wymant, *Eur. Phys. J. C* **74**, 10 (2014).
5. J. Y. Araz, M. Frank and B. Fuks, *Eur. Phys. J. C* **80**, 6 (2020).
6. M. Cacciari, G. P. Salam and G. Soyez, *JHEP* **04**, 063 (2008).
7. ATLAS Collaboration, *ATLAS-CONF-2018-038*, tech. rep. (July 2018).
8. B. Dumont, B. Fuks, S. Kraml *et al.*, *Eur. Phys. J. C* **75**, 2 (2015).
9. ATLAS Collaboration, M. Aaboud *et al.*, *JHEP* **12**, 034 (2017).
10. S. Ovyn, X. Rouby and V. Lemaître, `arXiv:0903.2225` (2010).
11. J. de Favereau, C. Delaere, P. Demin, A. Giammanco, V. Lemaître, A. Mertens and M. Selvaggi, *JHEP* **02**, 057 (2014).
12. M. Cacciari, G. P. Salam and G. Soyez, *Eur. Phys. J. C* **72**, 3 (2012).
13. A. L. Read, *J. Phys. G* **28**, 2693–2704 (2002).
14. C. Degrande, B. Fuks, V. Hirschi, J. Proudom and H.-S. Shao, *Phys. Lett. B* **755**, 82–87 (2016).
15. Wolfram Research, Inc., MATHEMATICA©, Version 12.0 (2021).
16. N. D. Christensen and C. Duhr, *Comput. Phys. Commun.* **180**, 1614–1641 (2009).
17. A. Alloul, N. D. Christensen, C. Degrande, C. Duhr and B. Fuks, *Comput. Phys. Commun.* **185**, 2250–2300 (2014).
18. J. Alwall, R. Frederix, S. Frixione, V. Hirschi, F. Maltoni, O. Mattelaer, H.-S. Shao, T. Stelzer, P. Torrielli and M. Zaro, *JHEP* **07**, 079 (2014).
19. R. Frederix, S. Frixione, V. Hirschi, D. Pagani, H.-S. Shao and M. Zaro, *JHEP* **07**, 185 (2018).
20. R. D. Ball, V. Bertone, S. Carrazza *et al.*, *Nucl. Phys. B* **867**, 244 (2013).

21. T. Sjöstrand, S. Ask, J. R. Christiansen, R. Corke, N. Desai, P. Ilten, S. Mrenna, S. Prestel, C. O. Rasmussen and P. Z. Skands, *Comput. Phys. Commun.* **191**, 159–177 (2015).
22. W. Beenakker, S. Brensing, M. Krämer, A. Kulesza, E. Laenen and I. Niessen, *JHEP* **12**, 041 (2009).
23. W. Beenakker, C. Borschensky, M. Krämer, A. Kulesza, E. Laenen, V. Theeuwes and S. Thewes, *JHEP* **12**, 023 (2014).
24. W. Beenakker, C. Borschensky, M. Krämer, A. Kulesza and E. Laenen, *JHEP* **12**, 133 (2016).
25. J. Butterworth *et al.*, *J. Phys. G* **43**, 023001 (2016).